

Optimizing the injection molding process for thermally and electrically conductive, carbon fiber and carbon nanotube-reinforced poly(lactic acid) hybrid composites with enhanced mechanical properties

Ábris Dávid Virág¹ | Csenge Tóth^{1,2} | László Mészáros^{1,3}  | Zsolt Juhász¹ |
 Ádám Bezerédi¹ | Roland Petrény¹

¹Department of Polymer Engineering, Faculty of Mechanical Engineering, Budapest University of Technology and Economics, Budapest, Hungary

²MTA-BME Lendület Lightweight Polymer Composites Research Group, Budapest, Hungary

³HUN-REN-BME Research Group for Composite Science and Technology, Budapest, Hungary

Correspondence

László Mészáros, Department of Polymer Engineering, Faculty of Mechanical Engineering, Budapest University of Technology and Economics, Műegyetem rkp. 3, H-1111, Budapest, Hungary.
 Email: meszaros@pt.bme.hu

Funding information

Nemzeti Kutatási, Fejlesztési és Innovációs Alap, Grant/Award Number: TKP-6-6/PALY-2021; Nemzeti Kutatási Fejlesztési és Innovációs Hivatal, Grant/Award Number: FK 138501; Magyar Tudományos Akadémia; National Research, Development and Innovation Office, Grant/Award Numbers: ÚNKP-23-3-II-BME-178, ÚNKP-23-3-II-BME-140, ÚNKP-23-5-BME-434

Abstract

We produced poly(lactic acid) (PLA) matrix carbon fiber and carbon nanotube-reinforced hybrid composites with enhanced thermal conductivity (0.48–0.59 W/mK) and electrical conductivity (0.35–0.97 S/cm). The conductive fillers greatly decreased the toughness, which was compensated with oligomeric lactic acid (OLA). Since fillers and plasticizers greatly alter the flow and thermal properties of the material as well, it was necessary to optimize several parameters of the injection molding process that were predetermined based on theoretical considerations. Based on oscillatory shear rheometry, we explored the rheological behavior of the materials in a wide temperature and shear rate range for the optimum injection molding temperatures, injection volume rates. We showed that by adding 15 wt% OLA as a plasticizer to the composites, the optimal processing temperature decreased by 45–135°C. This remarkable change illustrates the need for rheological studies of PLA compounds. The injection molded hybrid composites containing 5% oligomeric lactic had a tensile strength, modulus of elasticity, and work of fracture higher by 41%, 10%, and 150%, respectively, compared to samples without OLA.

KEYWORDS

biopolymers and renewable polymers, conducting polymers, fibers, graphene and fullerenes, nanotubes, plasticizer

1 | INTRODUCTION

In recent decades, there has been a growing focus on the research and development of biodegradable polymer composites and polymer composites of renewable

resources. Requirements for sustainability have prompted research on poly(lactic acid) (PLA). The properties of PLA can be optimized for a specific application if we combine PLA with other materials.¹ One of the main directions of research on PLA-based composites is the

This is an open access article under the terms of the [Creative Commons Attribution](https://creativecommons.org/licenses/by/4.0/) License, which permits use, distribution and reproduction in any medium, provided the original work is properly cited.

© 2024 The Author(s). *Journal of Applied Polymer Science* published by Wiley Periodicals LLC.

development of thermally and electrically conductive materials. The need for thermally conductive polymers is driven by the increasing energy density of electronic devices and the corresponding increasing cooling demand. The need for electrically conductive polymers is mainly seen in electromagnetic shielding and anti-static coatings, capacitors, fuel cells and medical devices. This is typically achieved with some form of conductive filler, like carbon nanotubes (CNT), or carbon fibers (CF), which must be present in the polymers in a volume fraction that ensures the formation of thermal and electrically conductive pathways. Of course, combining PLA and CF results in high-strength and high-modulus composites.^{2,3} Our previous studies showed that PLA matrix hybrid composites with CF and CNT have enhanced mechanical and functional properties. When CF are added besides CNTs, the shear stress increases during processing, which helps to disperse the CNTs properly and thus allows them to provide reinforcement.^{4,5} CNT enhance electrical conductivity⁶ and electromagnetic shielding⁷ if they are well dispersed in a PLA or PLA foam matrix.⁸ The combined effect of CFs and CNTs on electrical conductivity in hybrid composites has also been demonstrated.^{4,9}

However, the problem is that the PLA itself is rather brittle. Thus, the load-distributing potential of the matrix is not exploited—under load, shear stress is induced at the interface due to the modulus difference between the matrix and the fiber. The brittle matrix cannot absorb the deformation, so it separates from the fiber, resulting in failure. One way to delay the separation is to improve the interfacial adhesion between the fibers and the matrix. Studies have long demonstrated that surface modification techniques, for example, oxidation or plasma treatment can be used to enhance mechanical properties. Combined surface treatments can even improve the compatibility of natural fiber composites.¹⁰ Mina et al.¹¹ also showed that surface treatment of multi-walled CNTs also leads to improvements, as PLA reinforced with acid-treated CNTs exhibited improved tensile strength and modulus. Therefore, the conductive fillers often further reduce the elongation at break and the modulus and tensile strength as well, so good conductivity is at the expense of mechanical properties.¹² Conductive fillers not only cause a deterioration in mechanical properties but also affect the processing: conductive fillers tend to increase the viscosity of the material, which causes difficulties, particularly in melt processing such as extrusion or injection molding. PLA is also prone to degradation by increased temperatures and shear; therefore, lower temperatures and shear rates are preferred.¹³ Another problem is that both the matrix and the reinforcing materials have low coefficients of thermal expansion, which results in low shrinkage during cooling, and this

makes the product difficult to remove from the injection mold.¹⁴

The aforementioned issues can be solved by using various plasticizers. Plasticizers act as lubricants during processing: reduce viscosity, allow processing at lower pressures and temperatures, and improve impact resistance by toughening the matrix in a composite. Oligomeric lactic acid (OLA) is often used to improve the ductility of PLA and PLA-based composites.¹⁵ It comes from renewable resources, and due to similarities between their chemical structures, it is compatible with PLA and less prone to phase separation.¹⁶ The other condition for good compatibility is that there must be an appropriate viscosity ratio; otherwise, phase separation occurs.¹⁷ In the literature, OLA is typically mixed with PLA in a concentration of 5%–20%. Tejada-Oliveros et al.¹⁸ prepared PLA blends with dicumyl peroxide and OLA by reactive extrusion. The authors reported an increase in toughness with 10 wt% OLA content. Lascano et al.¹⁹ pointed out that with the right choice of injection molding parameters, a higher modulus can be achieved despite the plasticizing effect of OLA, and they reported a significant increase in impact strength at 15 wt% OLA content. However, the plasticizer also decreased elongation at break and tensile strength. Similarly, Avolio et al.²⁰ also found that plasticizing PLA with OLA is at the expense of tensile strength and modulus.

While conductive fillers generally increase viscosity and heat distortion temperature and reduce impact strength, plasticizers have the opposite effect. The combination of the two additives can enhance, weaken, or compensate for each other depending on how they are distributed in the matrix and the contact they establish with the matrix. The unexplored nature of this behavior not only affects the mechanical properties but can also cause problems during processing, for example, injection molding. Therefore, in order to determine processing parameters (such as melt temperature, injection speed, mold temperature or cooling time), the rheological and thermal behavior of the resulting material must first be known.

Our goal was to produce PLA-matrix hybrid composites containing CF and CNT. Our previous research showed that in CF/CNT hybrid composites, reinforcing materials have a synergistic effect, which improves both mechanical properties and conductivity.⁴ In this study, we aim to determine the optimal processing parameters while preserving the improved mechanical properties. For hybrid composites, the following must be ensured: proper distribution of the reinforcements and the plasticizers, and knowledge of rheological and thermal characteristics as a function of the additives. The first requirement assures the desired mechanical properties, while the latter can guarantee processing with reduced

thermal degradation. Knowledge of manufacturing criteria is crucial for mass production, which can broaden the range of applications for bio-based composites.

2 | MATERIALS AND METHODS

2.1 | Materials

We used PLA 4060D amorphous polylactic acid pellets manufactured by NatureWorks LLC, Plymouth, MN, USA, as the matrix for the composites. It has a density of 1.24 g/cm^3 , an MFI ($200^\circ\text{C}/2.16 \text{ kg}$) of $24.5 \text{ g}/10 \text{ min}^4$ and a D-lactide content of 12%–12.3%.⁸ According to the technical data sheet, the recommended processing temperature is between 190 and 210°C . As nanoscale reinforcement, we used Nanocyl NC7000 multi-wall CNT (Nanocyl S. A., Sambreville, Belgium) with a diameter of 9.5 nm , an average length of $1.5 \mu\text{m}$, and a specific surface area of $250\text{--}300 \text{ m}^2/\text{g}$. As micro-sized fibrous reinforcement, we applied chopped CF (Panex 35 chopped fiber (Type-95) supplied by Zoltek Zrt, Nyergesújfalú, Hungary) with a diameter of $8.3 \mu\text{m}$, a length of 6 mm , and a density of 1.81 g/cm^3 . Lastly, as a plasticizer, Glyplast OLA2 (Condensia, Barcelona, Spain) was used with a density of 1.10 g/cm^3 and a viscosity of $90 \text{ MPa}\cdot\text{s}$ at 40°C . To study the effect of the plasticizer, 3 different OLA contents were used. The weight fraction of each component is determined based on previous research,^{4,18,21} and the composition of the materials is shown in Figure 1.

2.2 | Processing and testing methods

2.2.1 | Extrusion

Before extrusion, the PLA pellets were dried for 4 h at 45°C , according to the recommendations of the manufacturer. A Thermolift 100–2 drying unit (Arburg GmbH, Loßburg, Germany) was used to dry the pellets, and then an

LTE 26–44 twin-screw extruder (Labtech Engineering, Samutprakarn, Thailand) (screw diameter: 26 mm , length/diameter (L/D) ratio: 44) and an LDF-1.6 liquid dosing system (Labtech Engineering, Samutprakarn, Thailand) were used to mix the OLA with the PLA. The filaments formed during the continuous extrusion were passed through an air-cooling conveyor belt to an LZ-120/VS pelletizer (Labtech Engineering, Samutprakarn, Thailand) to produce the pellets. First, the OLA was compounded with the PLA, with a screw speed of 40 rpm . The temperature profile from hopper to die was $180, 190, 190, 190, 190, 200, 200, 200, 200$, and 190°C . For materials with 10 and 15 wt% plasticizer content, the OLA was heated to 80°C for the required viscosity, and the melt temperatures were reduced by 30 and 40°C , respectively, which was necessary due to the decrease in viscosity. For the composites, the reinforcing materials were first dry mixed with the previously OLA-plasticized pellets and then compounded in a second extrusion step on the same twin-screw extruder. Figure 2 shows the compounding line.

2.2.2 | Hot pressing

We pressed $160 \times 160 \text{ mm}$, 2 mm -thick sheets with a PressPlate 200E (Dr. Collin GmbH, Munich, Germany) hydraulic press using a pressing temperature of 180°C . Pressing does not cause large shearing in the material like injection molding. First, the plates and the press frame were heated for 3 min. The pellets were then placed in the press frame for 1 min, then pressed at 0.625 MPa for 1 min, 1.25 MPa for 1 min and finally 2.5 MPa for 3 min. Between pressure increments, the compression die was opened for outgassing. The resulting sheet was cooled to room temperature under pressure.

2.2.3 | Dynamic rheological measurements

Dynamic rheology tests were performed with an MCR-301 (Anton-Paar, Graz, Austria) oscillatory shear

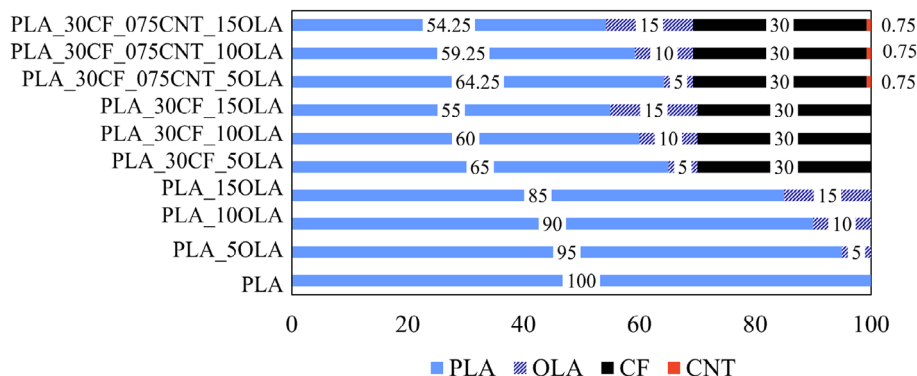


FIGURE 1 Composition of the materials. [Color figure can be viewed at wileyonlinelibrary.com]

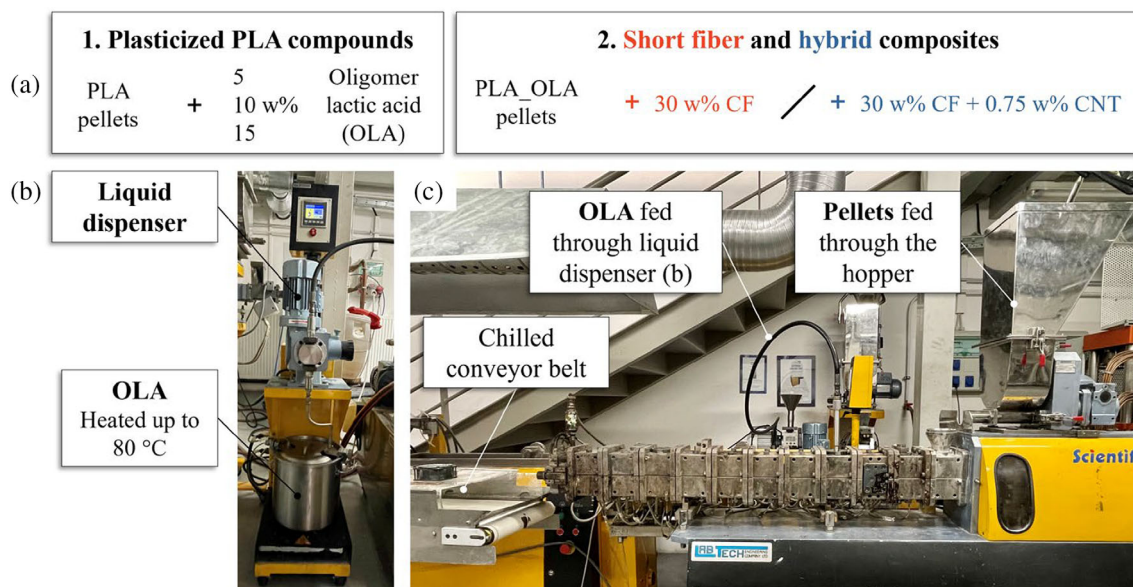


FIGURE 2 Compounding production line. [Color figure can be viewed at [wileyonlinelibrary.com](https://onlinelibrary.wiley.com/doi/10.1002/app.56148)]

rheometer in a parallel-plate geometry setup with a plate diameter of 25 mm and gap size of 1 mm and a Q800 dynamic mechanical analyzer (DMA) (TA instruments, New Castle, DE, USA) using a shear sandwich clamp. The tested samples were cut from the pressed sheets. Frequency sweeps were carried out in small amplitude oscillatory shear (SAOS) mode at several temperatures between 60 and 160°C, above the glass transition temperature (T_g) from 0.01 to 100 Hz. The amplitude of strain excitation was varied as a function of temperature for linear viscoelastic responses, which were verified by amplitude sweeps. Using the Q800 DMA, we also carried out temperature sweeps on 10 × 60 × 4 mm specimens cut out from the middle part of the injection molded specimens. The temperature range was 0–100°C with a heating rate of 2°C/min. The amplitude of deformation excitation was 0.1%, and the frequency was 1 Hz. The glass transition temperatures were determined based on the $\tan \delta$ peak.

2.2.4 | Thermal conductivity

The thermal conductivity was measured with a hot-plate conductivity meter on 80 × 80 × 4 mm press-molded sheets specimens. For this purpose, we used 2 pieces of the 2 mm thick sheets for each measurement, and for better heat transfer, heat-conducting paste was placed between the two samples and the sheets of the sample and the equipment. The lower plate of the apparatus was cooled by four Peltier cells. The upper plate was heated with a heating wire. This AlCr wire was 850 mm long, its diameter was 1 mm, and its nominal resistance was 1.5 Ω. The temperature was measured with two

thermistors on each side. When a steady state condition in heat flow is reached, measurement is simplified to one dimension, and Fourier's law can be used²²:

$$q(x, t) = -\lambda \cdot \nabla T(x, t), \quad (1)$$

where $q = 6$ [W] is the transmitted heat flux, λ [W/(m·K)] is thermal conductivity and ∇T [K] is the measured equilibrium temperature difference between the two plates.

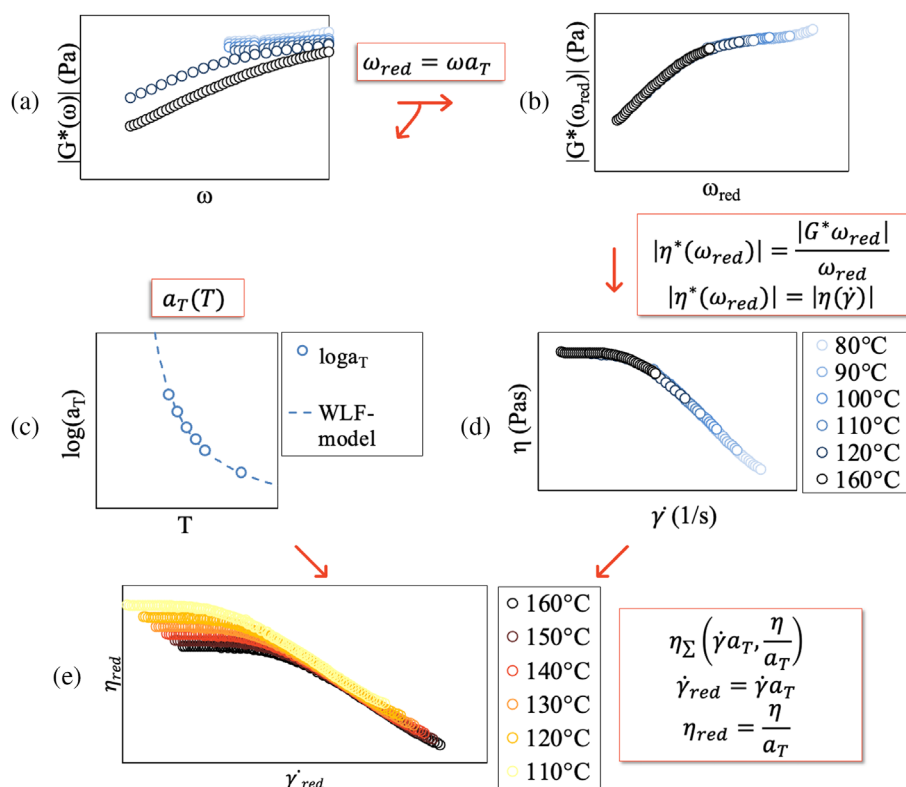
2.2.5 | Injection molding

Before injection molding, an Arburg Thermolift 100-2 drying unit (Arburg GmbH, Loßburg, Germany) was used to dry the pellets. The injection molding experiments were performed on an Allrounder 320C 400-170 injection molding machine (Arburg GmbH, Loßburg, Germany) with a mold tempering unit (Wittmann Technology GmbH, Wien, Austria). We used a two-cavity cold runner mold with a type 1A geometry according to the EN ISO 527 standard. The screw speed during plastification was 25 1/min. The other parameters of the injection molding process were determined for each material type, based on the measured rheological and thermal properties. These parameters are detailed in Section 3.1.1.

2.2.6 | Electrical conductivity

A four-pin resistance meter with an Agilent 34970A data logger was used to measure the electrical conductivity of

FIGURE 3 Method for determining the injection molding temperature. [Color figure can be viewed at wileyonlinelibrary.com]



the injection molded materials. The specific resistance of the materials was determined using Equation (2), c (cm) is the thickness of the sample, R is the measured resistivity, and G is electrical conductivity.²³

$$G\left(\frac{S}{cm}\right) = \frac{\ln(2)}{\pi \cdot c \cdot R}, \quad (2)$$

2.2.7 | Tensile test

The injection molded EN ISO 527 1A specimens were tensile tested on a Z020 tensile tester (Zwick GmbH, Ulm, Germany) using a 20 kN load cell with a resolution of 0.1 N and 20 kN-rated Zwick 8355 screw grips, with a grip length of 110 mm and a test speed of 2 mm/min. Five of each material were tested. For fracture work, the force-displacement curves were integrated.

2.2.8 | Scanning electron microscopy

Scanning electron microscope (SEM) micrographs were taken of the fracture surface perpendicular to the pulling direction of the tensile tested specimens with a JSM 6380LA SEM (JEOL, Tokyo, Japan) after the surface was sputtered with gold.

3 | RESULTS AND DISCUSSION

3.1 | Optimization of processing parameters

3.1.1 | Determination of the injection molding parameters

The content of reinforcing and plasticizing agents strongly influences the rheological and thermal properties of the materials to estimate shear rate-dependent viscosity over a wide range of shear rates, we used the method in Figure 3. For every unfilled OLA/PLA material, based on the method proposed by Virag et al.²⁴ a complex modulus master curve was constructed with the use of the time-temperature superposition (TTS) principle, described in detail by Ferry.²⁵

The complex modulus curves measured at different temperatures (Figure 3a) were reduced to an arbitrary reference temperature, $T_{ref} = 160^\circ\text{C}$ (Figure 3b). Then, the Williams-Landel-Ferry model (WLF model) (Equation 3)²⁶ was fitted to the resulting horizontal shift factors (a_T) (Figure 3c):

$$\log a_T = \frac{-c_1 \cdot (T - T_{ref})}{c_2 + (T - T_{ref})}, \quad (3)$$

where c_1 (1), c_2 (K) are empirical constants. The c_1 and c_2 constants were determined using the method of Oseli

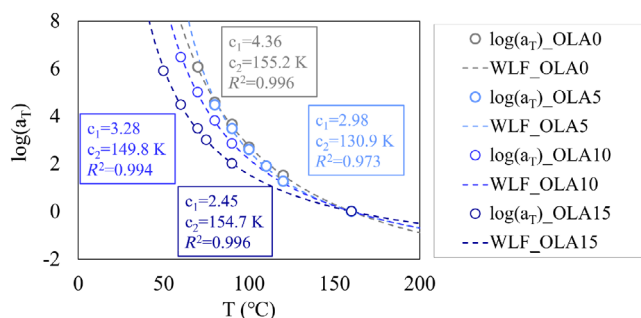


FIGURE 4 Temperature dependence of the shift factors for poly(lactic acid) with different oligomeric lactic acid content. [Color figure can be viewed at wileyonlinelibrary.com]

et al.²⁷ The method uses a two-dimensional coordinate system, where $x = T - T_{ref}$ and $y = \frac{T - T_{ref}}{\log a_T}$. The data were plotted in this coordinate system and a linear trend was fitted as $y(x) = mx + b$ to them (coefficients of determination (R^2) are shown in Figure 4). Then, the WLF constants were given as $c_1 = -\frac{1}{m}$ and $c_2 = \frac{b}{m}$.

The applied shift factors and the fitted WLF models are shown in Figure 4.

Then, we calculated the complex viscosity from the complex modulus according to Equation 4:

$$|\eta^*(\omega)| = \frac{|G^*(\omega)|}{\omega}, \quad (4)$$

The complex viscosity master curve $\eta^*(\omega)$ we obtained this way was converted to a shear flow viscosity curve $\eta(\dot{\gamma})$ assuming the Cox-Merz rule²⁸ (Equation 5) over the whole frequency range (Figure 3d):

$$|\eta^*(\omega)| = |\eta(\dot{\gamma})|, \quad (5)$$

After that, we estimated the shear rate-dependent viscosity at a given shear rate and temperature, $\eta_{\sum}(\dot{\gamma}_{red}, \eta_{red})$ (Figure 3e) using the $\dot{\gamma}_{red}$ reduced shear rate (Equation 6) and the η_{red} reduced viscosity (Equation 7):

$$\dot{\gamma}_{red} = \dot{\gamma} a_T, \quad (6)$$

$$\eta_{red} = \frac{\eta}{a_T}. \quad (7)$$

The initial parameters for the injection molding of the unfilled PLA were determined based on the literature,^{19,29} that is, the reference melt temperature for the neat PLA was set to 180°C, and the injection rate to 40 cm³/s. For injection rates of a few tens of cm³/s and a nozzle with a diameter of 2 mm, the shear rate is in the order of 10⁵ 1/s. Since the viscosity can be adjusted more easily and precisely by changing the temperature than by

varying the shear rate, we kept the shear rate constant and varied the temperature to achieve the desired viscosity. Figure 5a shows the viscosity curves of materials with different OLA contents for a temperature of 180°C. Our aim was to choose the injection molding temperature of each material in such a way that its viscosity curve coincides with the viscosity curve of pure PLA (OLA0) at 180°C, in the range of 10⁵ 1/s shear rate. Thus, using the temperature dependence of the displacement factors (fitted WLF models), based on Figure 3e, we reduced the temperature until the OLA5, OLA10, and OLA15 curves coincided with the neat PLA (OLA0) curve at $T = 180^\circ\text{C}$ in the shear rate range determined by the injection rate (Figure 5b). Based on these, the injection molding temperature was set to 165°C for OLA5, 145°C for OLA10, and 135°C for OLA15. These temperatures are far lower than the temperature range generally used to process PLA (180–200°C). The plasticizer significantly increases flowability (i.e., decreases viscosity); therefore, a much lower injection molding temperature is recommended. These temperatures were also used for the injection molding of the composite materials.

For the calculation of the required cooling time, it is important to know the glass transition temperature of the materials, as in the case of amorphous materials, this can be considered as the upper limit for the ejection temperature. Figure 6 shows that the use of OLA plasticizer in the PLA causes a slight reduction in the glass transition temperature. In this case, this is a positive effect, as we expect an increase in toughness with a reduction in T_g .

For the calculation of cooling time, the thermal conductivity and the specific heat capacity of the materials should be measured. The melt temperatures were calculated from the viscosity curves, and as the lowest glass transition temperatures for the materials plasticized with 15 wt% OLA were $\sim 38^\circ\text{C}$, we set the ejection temperature (T_{eject}) to 30°C to avoid the deformation of the final product. For this ejection temperature, mold temperature (T_{mold}) was chosen to be 25°C. Cooling time was calculated with Equation 7.³⁰:

$$t_{cooling} = \frac{h^2}{2\pi \cdot \alpha} \cdot \ln \left[\frac{4}{\pi} \left(\frac{T_{melt} - T_{mold}}{T_{eject} - T_{mold}} \right) \right], \quad (7)$$

where α is the thermal diffusivity, calculated with Equation 8:

$$\alpha = \frac{\lambda}{\rho \cdot c_p}, \quad (8)$$

where λ is thermal conductivity, ρ is density and c_p is specific heat.

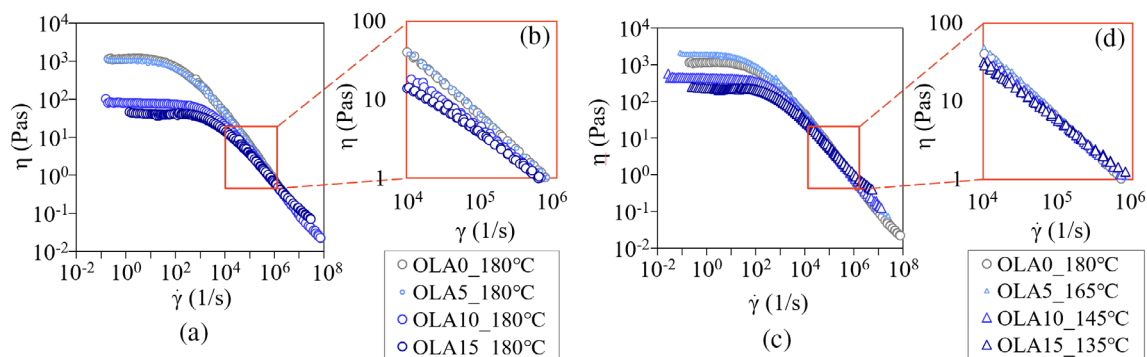


FIGURE 5 Viscosity curves of poly(lactic acid) with different oligomeric lactic acid contents at $T = 180^\circ\text{C}$ (a) and at different temperatures to coincide in the deformation speed range of injection molding (b). [Color figure can be viewed at wileyonlinelibrary.com]

FIGURE 6 Glass transition temperature in the pure, and in plasticized poly(lactic acid) (PLA), PLA + 30CF and PLA + 30CF + 075CNT materials. CNT, carbon nanotubes; CF, carbon fibers. [Color figure can be viewed at wileyonlinelibrary.com]

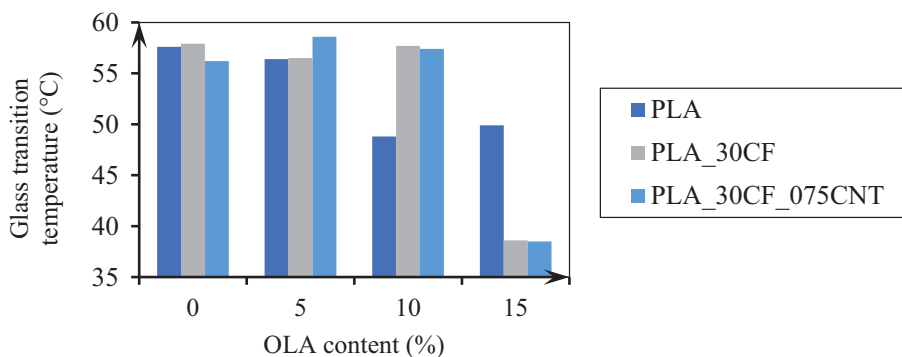
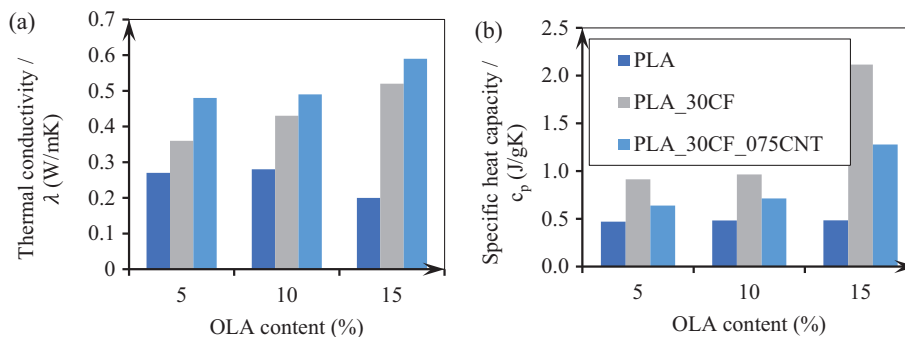


FIGURE 7 (a) Coefficient of thermal conductivity and (b) specific heat in the pure, and in the plasticized poly(lactic acid) (PLA), PLA + 30CF and PLA + 30CF + 075CNT materials. CNT, carbon nanotubes; CF, carbon fibers. [Color figure can be viewed at wileyonlinelibrary.com]



It can be observed in Figure 7 that the thermal conductivity of the carbon fiber composite is much higher compared with pure PLA, and the addition of CNT can further increase the thermal conductivity. This is explained by the fact that the CF in the injection molded material are unoriented and, therefore, cross each other at several points to form a thermal conductive network, while the CNT cross each other and the CF to form a secondary conductive network.^{4,31} In addition, the OLA content also has a thermal conductivity enhancing effect, presumably since the small molecules of the plasticizer are much more mobile and, therefore, more efficient in heat transfer. Increasing thermal conductivity is not only a well-explored functional property of materials but can

also make production more economical by shortening the injection molding cycle time.

The variation of the specific heat can be well correlated with the mobility of the polymer molecules: as shown in Figure 7, the reinforcing materials decreased the mobility of the PLA molecules, while the plasticizer increased it, and the specific heat varies in the same way as a function of the reinforcing material content and the plasticizer content.

The volume of the mold was 40 cm^3 , and the injection flow rate was $40\text{ cm}^3/\text{s}$, which resulted in an injection peak pressure of 1200 bar. With these parameters, smaller air voids were visible in the tensile specimens, so the injection rate was increased to $60\text{ cm}^3/\text{s}$, which increased

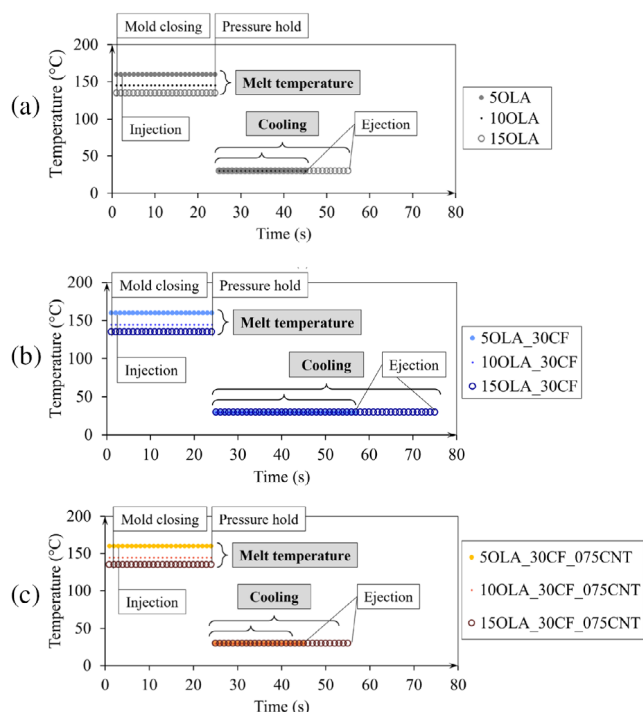


FIGURE 8 Injection molding cycles for (a) plasticized poly(lactic acid) (PLA), (b) plasticized fiber-reinforced PLA, and the (c) plasticized hybrid composites. [Color figure can be viewed at [wileyonlinelibrary.com](https://onlinelibrary.wiley.com)]

the peak pressure to 1600 bar, which made it possible for the holding pressure to increase to 600 bar. With the corrected parameters, the injection molded specimens were homogeneous without any air voids. The holding pressure was 600 bar and holding time was 20 s, according to the literature.³² Based on the determined parameters, Figure 7 shows the injection molding cycle diagrams. Even though OLA increased the thermal conductivity, the cycle time was longer because the plasticizer reduced the glass transition temperature and thus the heat retention of the product, so the cooling time was slower due to the lower ejection temperature. However, the use of hybrid reinforcing materials with higher thermal conductivity was able to compensate for this effect, so the shortest cycle times were obtained with hybrids (Figure 8).

3.2 | Electrical conductivity

Figure 9a shows that the addition of CNT to the carbon fiber-reinforced composites doubles the electrical conductivity of the material, which can be explained by the fact that the CNT form a secondary conductive path between the CF and connect them, resulting in a conductive network with higher conductivity in the composite. The

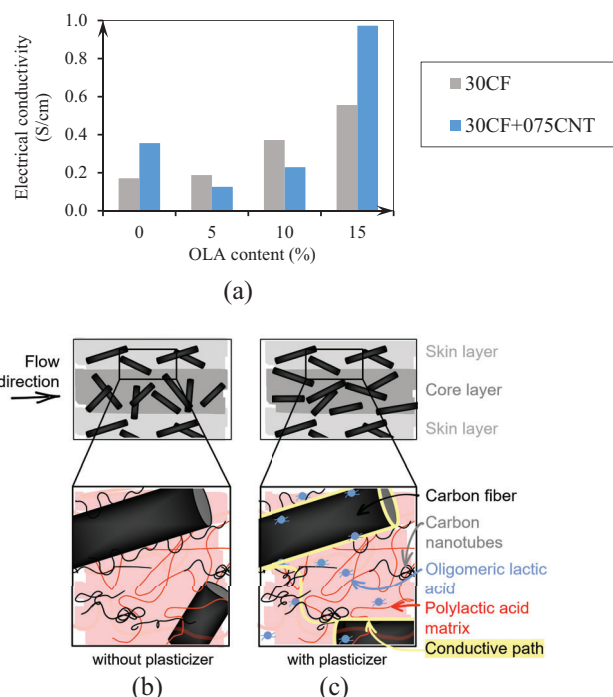


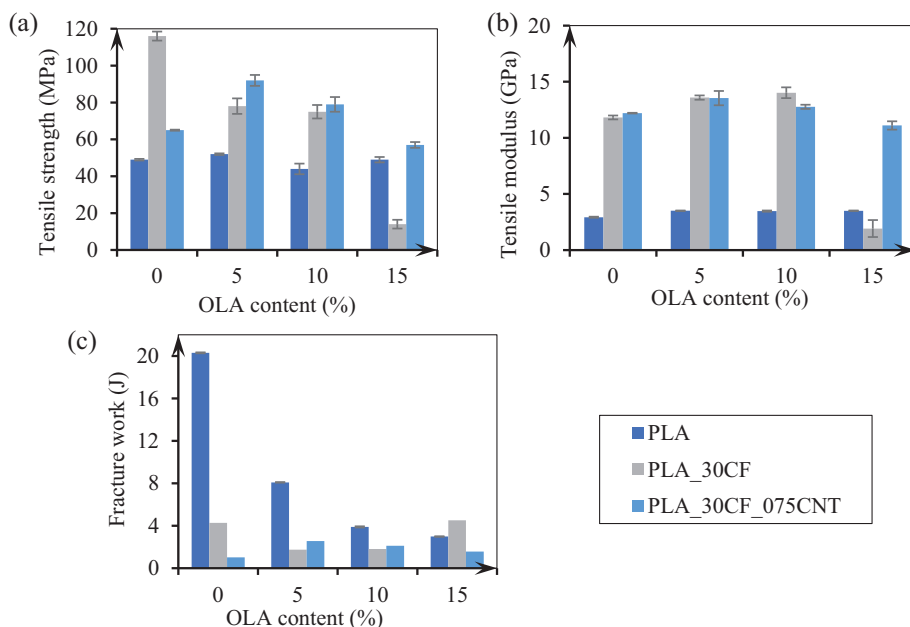
FIGURE 9 (a) Electrical conductivity in the pure, and in the plasticized PLA + 30CF and PLA + 30CF + 075CNT materials; schematics of the materials structure (b) without and (c) with oligomeric lactic acid plasticizer. PLA, poly(lactic acid); CNT, carbon nanotubes; CF, carbon fibers. [Color figure can be viewed at [wileyonlinelibrary.com](https://onlinelibrary.wiley.com)]

PLA_30CF_075CNT_15OLA material had an electrical conductivity of 0.97 S/cm, which is higher than commercially available conductive composites with conductivities between 0.1 and 0.6 S/cm.^{33–36} The OLA content increased the electrical conductivity of the materials, which can be explained by the fact that OLA helped the orientation of the carbon fiber during the injection molding process. Therefore, in our measurement setup, the conductivity in the longitudinal direction of the specimen increased with increasing OLA content. The presence of OLA not only helps the orientation but also breaks the nanotube-carbon fiber bonds because of the shear stress. At high OLA content, however, the shear stress between molecules is already reduced. Therefore, the orientation is easier to achieve, but the nanotubes do not separate from the CF. The conducting network is preserved, and thus, a kind of synergy in electrical conductivity is awakened (Figure 9c).

3.3 | Mechanical properties

The unplasticized composites containing carbon fiber and CNT became very brittle due to the conductive fillers. However, in the hybrid composites plasticized

FIGURE 10 Tensile properties of the materials (a) tensile strength, (b) tensile modulus, and (c) fracture work. [Color figure can be viewed at [wileyonlinelibrary.com](https://onlinelibrary.wiley.com/doi/10.1002/app.56148)]



with OLA, both tensile strength and tensile modulus significantly increased compared to the unplasticized hybrids. A possible cause is the better load transfer of the tougher matrix material toward the reinforcing fibers. The work of fracture calculated from the force–strain curves measured during the tensile tests (Figure 10) shows that the addition of a plasticizer to the hybrid composite increased its toughness. The highest increase in toughness was obtained with a concentration of 5 wt% OLA. Commercially available conductive materials typically have a modulus of around 5 GPa, while their tensile strength typically ranges from 50 to 105 MPa.^{34,36,37} Figure 10 shows that our PLA-based composites containing 30% carbon fiber and 0.75% CNT all have tensile strengths above 60 MPa and modulus above 10 GPa, so in addition to excellent conductivity, strength properties are equal to or higher than those of commercially available materials.

Figure 11 shows the areas under the glass transition peak of the $\tan \delta$ curves measured with DMA, the magnitude of which is proportional to the materials' energy absorption capacity. The conductive reinforcing materials caused the area under the peak to decrease significantly. The addition of the plasticizer allowed the area under the peak to return to close to the reference PLA value and even exceeded it for the material containing 15% OLA.

3.4 | Scanning electron microscopy

The OLA resulted in more structured fracture surfaces, and the crack path is also longer, indicating increased

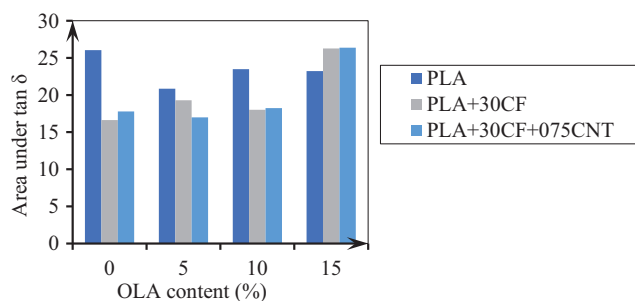


FIGURE 11 Energy absorbing capability of the materials. [Color figure can be viewed at [wileyonlinelibrary.com](https://onlinelibrary.wiley.com/doi/10.1002/app.56148)]

plastic deformation (Figure 12a–d).³⁸ In the CF-reinforced composite specimens, the increase in OLA concentration results in higher plastic deformation during rupture due to the softening effect (Figure 12e–h).³⁹ As the OLA content increases, longer and longer free-standing fibers can be seen on the surface of the fragment. This suggests either that the OLA is enriched near the interface, which is most likely when OLA content is high. In SEM images of hybrid composites with CNTs, the fracture surface is significantly different with 5 or 15 wt% OLA content (Figure 12i–l). The fracture surface is very similar, which may indicate that the nanotubes can transfer the load well from the matrix material to the CF, even at high OLA content. This is also illustrated by the fact that more fiber breaks are visible in nanotube-reinforced samples, and there are matrix residues on the fibers, suggesting improved fiber–matrix adhesion (Figure 9l).

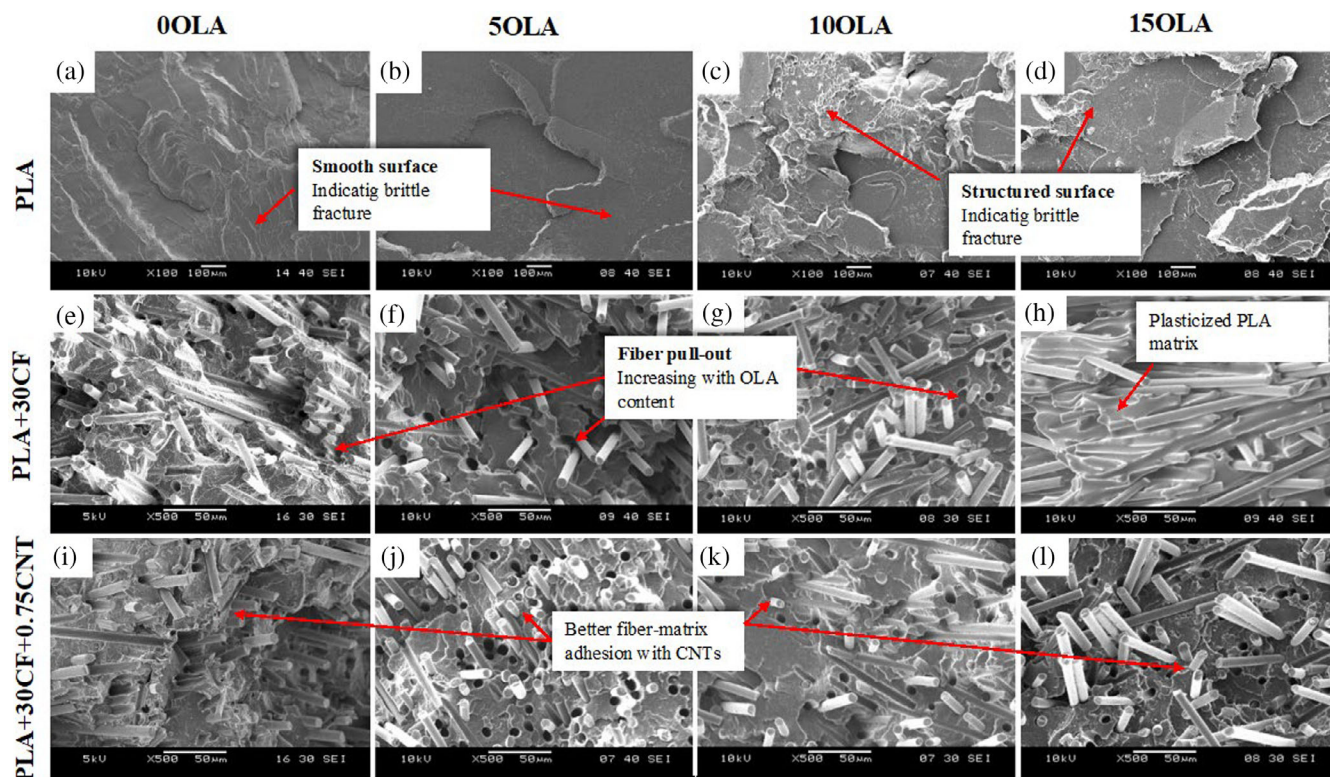


FIGURE 12 SEM images of the fracture surfaces of the (a–d) pure poly(lactic acid) (PLA), (e–f) CF-reinforced PLA composites, and (i–l) PLA hybrid composites reinforced by CF and CNT. CNT, carbon nanotubes; CF, carbon fibers. [Color figure can be viewed at [wileyonlinelibrary.com](https://onlinelibrary.wiley.com/doi/10.1002/app.56148)]

4 | CONCLUSION

We produced thermally and electrically conductive hybrid composites with a PLA matrix reinforced with carbon fiber and CNT. The conductive fillers resulted in a large decrease in toughness, which was compensated with OLA. Oscillatory shear rheometry was applied to determine the rheological behavior of the materials in a wide temperature and shear rate range. Using the shear rate and temperature dependence of the viscosity, the glass transition temperature, thermal conductivity and the specific heat as input parameters, we determined the injection molding temperatures, injection flow rates and cycle times for each material to produce the composites. We showed that by adding 15 wt% OLA plasticizer to the composites, the optimal processing temperature decreased by 45°C, and due to the good thermal conductivity of the hybrid composites, the required cooling time was decreased. The injection molded hybrid composites containing CF and CNT had thermal conductivities between 0.48 and 0.59 W/mK and electrical conductivities between 0.35 and 0.97 S/cm, with tensile strengths above 60 MPa and modulus above 10 MPa, so that in addition to excellent conductivity, strength properties are

equal to or higher than those of commercially available materials.

AUTHOR CONTRIBUTIONS

Ábris Dávid Virág: Conceptualization (equal); investigation (equal); methodology (equal); validation (equal); visualization (equal); writing – original draft (equal). **Csenge Tóth:** Data curation (equal); validation (equal); visualization (equal); writing – original draft (equal). **László Mészáros:** Conceptualization (equal); methodology (equal); supervision (equal); writing – review and editing (equal). **Zsolt Juhász:** Investigation (equal); validation (equal). **Ádám Bezerédi:** Investigation (equal); validation (equal); visualization (equal). **Roland Petrény:** Conceptualization (equal); investigation (equal); methodology (equal); supervision (equal); validation (equal); writing – original draft (equal); writing – review and editing (equal).

ACKNOWLEDGMENTS

Project no. TKP-6-6/PALY-2021 has been implemented with the support provided by the Ministry of Culture and Innovation of Hungary from the National Research, Development, and Innovation Fund, financed under the

TKP2021-NVA funding scheme. László Mészáros is thankful for the János Bolyai Research Scholarship of the Hungarian Academy of Sciences. The research reported in this paper was supported by the National Research, Development and Innovation Office (FK 138501). Ábris Dávid Virág is thankful for the support of the ÚNKP-23-3-II-BME-178, Csenge Tóth for the support of the ÚNKP-23-3-II-BME-140 and László Mészáros for the support of the ÚNKP-23-5-BME-434 New National Excellence Program of the Ministry for Culture and Innovation from the source of the National Research, Development and Innovation Fund.

DATA AVAILABILITY STATEMENT

The data that support the findings of this study are available from the corresponding author upon reasonable request.

ORCID

László Mészáros  <https://orcid.org/0000-0001-5979-7403>

REFERENCES

- [1] S. Liu, S. Qin, M. He, D. Zhou, Q. Qin, H. Wang, *Compos. Part B Eng.* **2020**, *199*, 108238.
- [2] Y. Zhou, L. Lei, B. Yang, J. Li, J. Ren, *Polym. Test.* **2018**, *68*, 34.
- [3] H. Barangizi, J. Krajenta, A. Pawlak, *Express Polym Lett* **2023**, *17*, 738.
- [4] R. Petrényi, C. Tóth, A. Horváth, L. Mészáros, *Heliyon* **2022**, *8*, e10287.
- [5] Y. Wang, Y. Mei, Q. Wang, W. Wei, F. Huang, Y. Li, J. Li, Z. Zhou, *Compos. Part B Eng.* **2019**, *162*, 54.
- [6] Y. Wang, C. Yang, Z. Xin, Y. Luo, B. Wang, X. Feng, Z. Mao, X. Sui, *Compos. Commun.* **2022**, *30*, 101087.
- [7] Y. Wang, Z.-W. Fan, H. Zhang, J. Guo, D.-X. Yan, S. Wang, K. Dai, Z.-M. Li, *Mater. Des.* **2021**, *197*, 109222.
- [8] T. Standau, C. Zhao, S. Murillo Castellón, C. Bonten, V. Altstädt, *Polymers* **2019**, *11*, 306.
- [9] H. Wang, J. Tao, K. Jin, X. Wang, Y. Dong, *Compos. Part A Appl. Sci. Manuf.* **2022**, *154*, 106796.
- [10] J. O. Akindoyo, M. D. H. Beg, S. Ghazali, M. R. Islam, *J. Appl. Polym. Sci.* **2015**, *132*, 132.
- [11] M. F. Mina, M. D. H. Beg, M. R. Islam, A. Nizam, A. K. M. M. Alam, R. M. Yunus, *Polym. Eng. Sci.* **2014**, *54*, 317.
- [12] D. Sheela, B. Retnam, M. Sivapragash, *Int. J. Mech. Eng. Technol.* **2018**, *9*, 779.
- [13] M. Oliveira, E. Santos, A. Araújo, G. J. M. Fachine, A. V. Machado, G. Botelho, *Polym. Test.* **2016**, *51*, 109.
- [14] S. Kuciel, K. Mazur, M. Hebda, *J. Polym. Environ.* **2020**, *28*, 1204.
- [15] Y. Qu, J. Hong, Y. Chen, X. Ling, J. Wu, H. Wang, Y. Li, *Compos. Part B Eng.* **2023**, *255*, 110619.
- [16] K. Litauski, R. Petrényi, Z. Haramia, L. Mészáros, *Heliyon* **2023**, *9*, e14674.
- [17] N. Furguele, A. H. Lebovitz, K. Khait, J. M. Torkelson, *Polym. Eng. Sci.* **2000**, *40*, 1447.
- [18] R. Tejada-Oliveros, S. Fiori, J. Gomez-Caturra, D. Lascano, N. Montanes, L. Quiles-Carrillo, D. Garcia-Sanoguera, *Polymers* **2022**, *14*, 14.
- [19] D. Lascano, G. Moraga, J. Ivorra-Martinez, S. Rojas-Lema, S. Torres-Giner, R. Balart, T. Boronat, L. Quiles-Carrillo, *Polymers* **2019**, *11*, 11.
- [20] R. Avolio, R. Castaldo, G. Gentile, V. Ambrogio, S. Fiori, M. Avella, M. Cocca, M. E. Errico, *Eur. Polym. J.* **2015**, *66*, 533.
- [21] L. Mészáros, A. Horváth, L. M. Vas, R. Petrényi, *Compos. Sci. Technol.* **2023**, *242*, 110154.
- [22] A. Suplicz, J. G. Kovács, *Mater. Sci. Forum* **2013**, *729*, 80.
- [23] J. Cinquin, C. Heinrich, E. Balland, F. Pons, Volume electrical conductivity measurement on organic composite material, *Proceeding of SAMPE-SETEC*. **2013**.
- [24] Á. D. Virág, Z. Juhász, A. Kossa, K. Molnár, *Polymer* **2024**, *295*, 126742.
- [25] J. D. Ferry, H. S. Myers, *J. Electrochem. Soc.* **1961**, *108*, 142C.
- [26] M. L. Williams, R. F. Landel, J. D. Ferry, *J. Am. Chem. Soc.* **1955**, *77*, 3701.
- [27] A. Oseli, A. Aulova, M. Gergesova, I. Emri, in *Effect of Temperature on Mechanical Properties of Polymers BT - Encyclopedia of Continuum Mechanics* (Eds: H. Altenbach, A. Öchsner), Springer, Berlin, Heidelberg **2019**, p. 1. https://doi.org/10.1007/978-3-662-53605-6_269-2
- [28] W. P. Cox, E. H. Merz, *J. Polym. Sci.* **1958**, *28*, 619.
- [29] T. Tábi, T. Ageyeva, J. G. Kovács, *Mater. Today Commun.* **2022**, *32*, 103936.
- [30] J. Z. Liang, J. N. Ness, *J. Mater. Process. Technol.* **1996**, *57*, 62.
- [31] Z. Fang, M. Li, S. Wang, Y. Gu, Y. Li, Z. Zhang, *Int. J. Heat Mass Transf.* **2019**, *137*, 1103.
- [32] T. Tábi, T. Ageyeva, J. G. Kovács, *Polym. Test.* **2021**, *101*, 107282.
- [33] J. Santo, P. K. Penumakala, *J. Manuf. Process.* **2023**, *108*, 513.
- [34] J. Santo, P. K. Penumakala, R. B. Adusumalli, *Polym. Compos.* **2021**, *42*, 3231.
- [35] J.-R. Tao, C.-L. Luo, M.-L. Huang, Y.-X. Weng, M. Wang, *Compos. Part A Appl. Sci. Manuf.* **2023**, *164*, 107304.
- [36] X. Zhou, L. Wu, J. Wang, *Compos. Part A Appl. Sci. Manuf.* **2023**, *174*, 107739.
- [37] Q.-Y. Wei, Y.-D. Fang, Z.-B. Sun, Y. Zeng, J. Zhang, J. Lei, L. Xu, H. Lin, G.-J. Zhong, Z.-M. Li, *Compos. Part A Appl. Sci. Manuf.* **2023**, *169*, 107516.
- [38] Y. Qin, Y. Wang, Y. Wu, Y. Zhang, H. Li, M. Yuan, *J. Polym. Environ.* **2014**, *23*, 374.
- [39] M. Murariu, Y. Paint, O. Murariu, F. Laoutid, P. Dubois, *Polymers* **2022**, *14*, 4836.

How to cite this article: Ábris Dávid Virág, C. Tóth, L. Mészáros, Z. Juhász, Á. Bezerédi, R. Petrényi, *J. Appl. Polym. Sci.* **2024**, e56148. <https://doi.org/10.1002/app.56148>